

Original Article

DOI 10.1007/s12206-020-0722-2

Keywords:

- Electrostatic precipitator
- Computational fluid dynamics (CFD)
- Air cleaning
- Corona discharge
- Charging model
- Discrete phase model (DPM)

Correspondence to:

Yong Gap Park
pyg777@changwon.ac.kr
Mang Yeong Ha
myha@pusan.ac.kr

Citation:

Choi, H. Y., Park, Y. G., Ha, M. Y. (2020). Numerical study on the effect of staggered wire electrodes in an electrostatic precipitator. *Journal of Mechanical Science and Technology* 34 (8) (2020) 3303–3310.
<http://doi.org/10.1007/s12206-020-0722-2>

Received September 23rd, 2019

Revised January 29th, 2020

Accepted February 20th, 2020

† This paper was presented at AUKFluids2019, Hyatt Regency, San Francisco, CA, USA, July 28 - August 1, 2019. Recommended by Guest Editor Seongwon Kang and Hyoung-gwon Choi

Numerical study on the effect of staggered wire electrodes in an electrostatic precipitator

Ho Yeon Choi¹, Yong Gap Park² and Man Yeong Ha¹

¹School of Mechanical Engineering, Pusan National University, 2, Busandaehak-ro 63beon-gil, Geumjeong-gu, Busan 46241, Korea, ²School of Mechanical Engineering, Changwon National University, 20 Changwondaehak-ro, Uichang-gu, Changwon-si, Gyeongsangnam-do, Korea

Abstract In this paper, a numerical model is developed to describe the wire-plate electrostatic precipitator used in industrial application for air cleaning. The complex interactions between fluid dynamics, electric fields and particle dynamics are considered. Therefore, the combined Eulerian and Lagrangian approach is used in this study. In order to describe corona phenomena around high voltage electrode, electric field and ion current density field in electrostatic precipitator are numerically calculated using the iterative method for corona discharge model suggested by Kim [1]. The charging model suggested by Lawless [2] is used for the charging phenomena of particles by corona discharge because it was designed to predict combination effect of diffusion charge and field charge. The numerical model in this study is implemented by UDF in commercial software FLUENT and validated with experimental and numerical results from literatures. The effects of wire arrangement on electrostatic precipitator characteristics are investigated. Both inline and staggered arrangements of wire electrode have been considered for fixed value of gas velocity equal to 2 m/s. Applied voltage on wire electrode is varied in the range of 6 to 13 kV and particle diameter is 4 μm . For low voltage condition, staggered arrangement of wire electrode caused the turbulent effect so that the collection efficiency increases more than inline arrangement. However, the collection efficiency decreases in high voltage condition because electric force applied on particles passing between the wire electrodes is canceled out by both side wire electrodes.

1. Introduction

Due to the rapid industrial and urban developments in many cities around the world, fine particle emissions are definitely among the most serious environment problems, which may cause great health hazards to people.

Over the years, electrostatic precipitators are most widely used in industries for removing particles from gases, mainly due to its higher efficiency, lower resistance and wider adaptability to various kinds of dust particles. Recently, the electrostatic precipitation technology has been used in air purifier, and the use of air purifiers for air purification has increased rapidly in indoor environment such as offices, hospitals, and houses. However, with increasingly strict regulations on fine suspended particles emission in all industries, the performance of electrostatic precipitators are must be improved, and the charging and collection mechanisms of particles in electrostatic precipitators also need to be further investigated.

The electrostatic precipitation involves three highly related physical fields of gas flow, electrostatics, and particle motions. Because of complexity of precipitation phenomenon, conventional analysis on removing particles process was mainly based on simplified theories and empirical correlations such as the Deutsch equation [3] and the theories of Cooperman [4] and Leonard et al. [5]. However, with the developments of numerical approaches to analyze physical phenomenon, more comprehensive and advanced models have been proposed and developed to

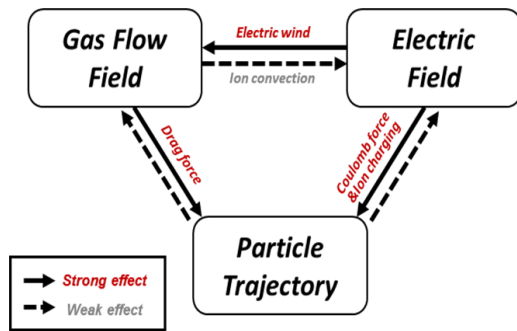


Fig. 1. Interaction of physical system in electrostatic precipitator.

evaluate performance of electrostatic precipitators. One of the first numerical method on solving the electric field with corona discharge in the electrostatic precipitators was suggested by McDonald [6]. And numerical model for coupling of gas flow and electric fields was developed by Kim [1]. Since then, Nikas [7] and Goo and Lee [8] developed the numerical models with consideration of particle charging dynamics using charging models proposed by Smith and McDonald [9] and White [10]. Recently, Adamiak and Atten [11] suggested a coupled numerical model for the simulation of secondary EHD flows caused by corona discharge and charged particles.

Multi-wire electrodes are designed to improve the collection efficiency in the electrostatic precipitator in industrial applications, and the majority of most previous studies were only focused on the design of the inline arrangement of wire electrodes [12-18]. In this study, the effect of wire arrangement in electrostatic precipitator characteristics and particle charging are investigated. Both inline and staggered arrangements of wire electrode have been considered for fixed value of gas velocity equal to 2 m/s. Applied voltage on wire electrode is varied 6 to 13 kV and particle diameter is 4 μm based on Kihm's experiment [16].

2. Numerical methodology

The numerical modeling of an electrostatic precipitator involves physical phenomena which are interacted electric field, turbulent flow field, particle charging and motion of particles simultaneously. So, the influence of gas flow characteristics, namely the velocity distributions, turbulent factors, as well as the ionic wind from electric field can be considered in the electrostatic precipitator simulation as shown in Fig. 1. The commercial CFD software ANSYS FLUENT is used for this simulation. The interaction between electric field, flow field and particle motion is implemented by user define functions, ANSYS FLUENT capability. The electrostatic precipitator with simple geometry, which called wire-plate type and commonly used in industries, is used in this simulation. The computational domain was simplified to 2 dimensions.

2.1 Gas flow field

The advantages of an electrostatic precipitator are small

Table 1. Boundary conditions of electrostatic precipitator.

	Gas velocity	Electric potential	Ion current density	Particle motion
Inlet	$U = 2 \text{ m/s}$	$\frac{\partial \varphi}{\partial n} = 0$	$\frac{\partial \rho_{ion}}{\partial n} = 0$	$u_p = 2 \text{ m/s}$
Outlet	Pressure outlet	$\frac{\partial \varphi}{\partial n} = 0$	$\frac{\partial \rho_{ion}}{\partial n} = 0$	Escape
Collection plate	No slip	$\varphi = 0$	$\frac{\partial \rho_{ion}}{\partial n} = 0$	Trap
Wire electrode	No slip	$\varphi = \varphi_w$	$\rho_{ion} = \rho_{ion,w}$	Reflect

pressure loss and temperature gradient. Therefore the gas flow inside electrostatic precipitator can be treated as incompressible flow and can be described as the conservation of mass and momentum equations as follows:

$$\frac{\partial}{\partial x_k}(\rho u_k) = 0 \quad (1)$$

$$\frac{\partial}{\partial x_k} \left(\rho u_k u_k - (\mu + \mu_t) \frac{\partial u_i}{\partial x_k} \right) = -\frac{\partial P}{\partial x_i} + F_e \quad (2)$$

where $F_e = \rho_{ion} E_k$ is the term of electric body force. Due to momentum transport by the ion current density and electric potential fields, the term of electric body force is caused the secondary flow in gas flow field and is effected to particle motion. The turbulence kinetic viscosity in Eq. (2) was calculated with the k - ε turbulence model as follows:

$$\frac{\partial}{\partial t}(\rho k) + \frac{\partial}{\partial x_i}(\rho u_i k) = \frac{\partial}{\partial x_j} \left(\frac{\mu_t}{\sigma_k} \frac{\partial k}{\partial x_j} \right) + 2\mu_t G - \rho \varepsilon \quad (3)$$

$$\frac{\partial}{\partial t}(\rho \varepsilon) + \frac{\partial}{\partial x_i}(\rho u_i \varepsilon) = \frac{\partial}{\partial x_j} \left(\frac{\mu_t}{\sigma_\varepsilon} \frac{\partial \varepsilon}{\partial x_j} \right) + C_1 \frac{\varepsilon}{k} 2\mu_t G - \rho C_2 \frac{\varepsilon^2}{k} \quad (4)$$

$$G = \frac{1}{2} \frac{\partial}{\partial x_j} \left(\frac{\partial u_i}{\partial x_j} + \frac{\partial u_j}{\partial x_i} \right) \frac{\partial u_i}{\partial x_j} \quad (5)$$

$$\mu_t = \rho C \frac{\varepsilon^2}{k} \quad (6)$$

2.2 Electric field

The electric field in electrostatic precipitator is governed by Poisson's equation and is expressed in the terms of electric potential and ion current density as follows:

$$\frac{\partial^2 \varphi}{\partial x_k^2} = -\frac{\rho_{ion}}{\varepsilon_0} \quad (7)$$

The ion current density is governed by the convection-diffusion equation as:

$$\frac{\partial}{\partial x_k} \left[\rho_{ion} (k_{ion} E_k + u_k) - D_e \frac{\partial \rho_{ion}}{\partial x_k} \right] = 0 \tag{8}$$

$$E_k = -\frac{\partial \phi}{\partial x_k} \tag{9}$$

where k_{ion} is the ion mobility of negative [13], D_e is the ion diffusivity [13], E_k is the electric field strength, respectively. E_k is main factor of momentum transport from ionic field to gas flow.

These equations are subjected to certain boundary conditions. The value of boundary condition for governing equations is given in Table 1.

In addition, the Peek's law is satisfied to determine the corona onset on the wire electrode, thus the corona onset electric strength can be determined following as:

$$E_s = 3.1 \times 10^6 \delta \left(1 + \frac{0.03}{\sqrt{\delta r}} \right) \tag{10}$$

2.3 Particle dynamics and charging

Since the particulate two-phase flow in electrostatic precipitator is evenly floated, the Lagrangian approach is used for particle trajectories. The Lagrangian approach could present a more accurate description of the particle motion and charging process, as well as the collection efficiency of electrostatic precipitators compared with the Eulerian approach. In this study, the discrete phase model (DPM) that can predict the trajectory of the particle by integrating the force balance on the particle in the Lagrangian reference frame is employed to solve the particle tracking in the ESP. As a result of comparing the magnitudes of the forces acting on the particles, particles are dominantly subjected to aerodynamics drag and electric forces, and the governing equation of the particle dynamics is described as:

$$\frac{d\vec{u}_p}{dt} = C_D \frac{3\rho |\vec{u}_i - \vec{u}_p| (\vec{u}_i - \vec{u}_p)}{4\rho_p d_p} + F_{coul} \tag{11}$$

$$F_{coul} = \frac{Eq_p}{m_p} = \frac{3Eq_p}{4\rho_p d_p^3} \tag{12}$$

where F_{coul} is coulomb force on the particles caused by electric field, and is main factor of collecting behavior.

A charging of particles is usually described two distinct mechanisms: diffusion charging and field charging. Diffusion charging is considered for small particle or low electric fields. Field charging is considered for large particles and high electric fields. In intermediate region where is affected by both diffusion and field charging, charging model which considered only diffusion charging or field charging is not adequate and should be replaced by combined model of two mechanisms. In this study, the combined charging model developed by Lawless [2] is used for accurate charging phenomena of particles. Lawless's

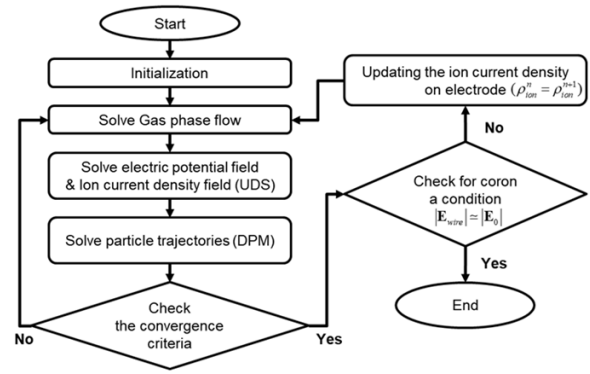


Fig. 2. Flow chart of electrostatic precipitator simulation.

charging model is expressed in a dimensionless formula as:

$$\frac{dv}{dt_q} = \begin{cases} f(w) \frac{v-3v}{\exp(v-3v)-1}, & v > 3w \\ \frac{3w}{4} \left(1 - \frac{w}{3w} \right)^2 + f(w), & -3w \leq v \leq 3w \\ -v + f(w) \frac{-v-3v}{\exp(v-3v)-1}, & v < -3w \end{cases} \tag{13}$$

$$f(w) = \begin{cases} \frac{1}{(w+0.475)^{0.575}}, & w \geq 0.525 \\ 1, & w < 0.525 \end{cases} \tag{14}$$

where $v = q_p e / 2\pi \epsilon_0 d_p k_b T$ is the dimensionless particle charge, $w = (K_p / K_p + 2) (Ed_p e / 2k_b T)$ is the dimensionless electric field strength, and $t_q = \rho_s k_{ion} t / \epsilon_0$ is the dimensionless charging time. $f(w)$ is the area fraction of particle surface covered by diffusion band.

Fig. 2 shows the flow chart of electrostatic precipitator simulation processes. The algorithm has been arranged into two iterative loops. For a given ion current density on the wire electrode, whole governing equations are solved for the physical variables in the whole computational domain until convergence is reached. In the outer iterative loop the ion current density on wire electrode is updated. This step is needed in order to satisfy corona onset determined from the Peek's law. The ion current density on the wire electrode is iterated until the electric strength is sufficiently close to corona onset value.

3. Results and discussion

3.1 Validation with previous experimental data

To verify and validate the numerical simulation using present model, calculation of corona electric field was first conducted and compared with the experimental data of Penney and Matick [14]. Fig. 3 shows the schematic of electrostatic precipitator used in Penney and Matick's experiment. The electric potential and ion current density field were calculated

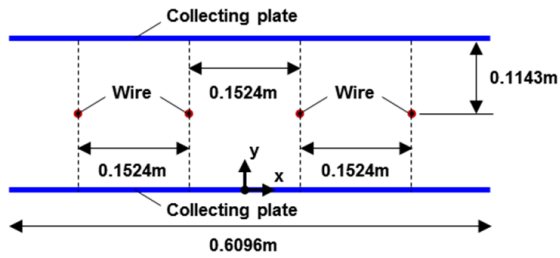


Fig. 3. Schematic of the electrostatic precipitator used by Penny and Matick [14].

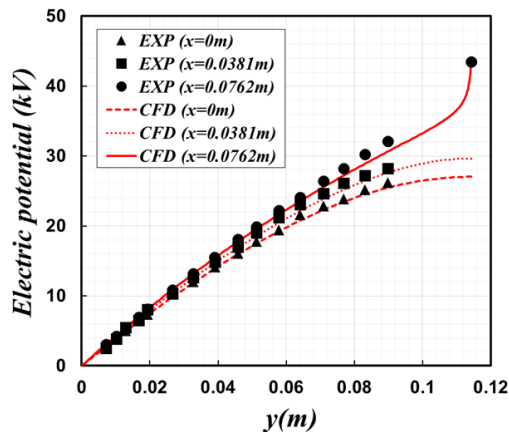


Fig. 4. Comparison of electric potential distributions between present CFD and experiment of Penney and Matick [14].

for electrostatic precipitator with four wire electrode of 300 μm diameter and applied voltage of 43.5 kV on wire electrode. The electric potential distributions from collecting plate to the center-line in y -direction at $x = 0$, $x = 0.0381$ m and $x = 0.0762$ m are compared with the experimental results of Penney and Matick [14]. As shown in Fig. 4, the calculated distributions of electric potential are in good agreement with experimental results when corona discharge is occurred. Numerical simulation of electric field has been validated with Penney and Matick's experiment.

Second validation was carried out to compare the results of present model with experimental data measured by Parasram [15] for current density distribution on the collection plate and transverse particle velocity near the collection plate. Fig. 5 shows the schematic of electrostatic precipitator used in Parasram's experiments. The electrostatic precipitator has three wire electrode with diameter of 50 μm and applied voltage for corona discharge is 15 kV. Inlet velocity of gas flow is 1 m/s.

In Fig. 6(a), the current density on the collection plate found to be in good agreement with experimental data. That means electric fields is very well predicted in numerical simulation. Fig. 6(b) shows the transverse particle velocities along the flow direction at $y = 5$ mm from collection plate. The transverse particle velocities increase near the wire electrodes due to the strong electric strength. Then, the transverse particle velocities decrease near the halfway between the wire electrodes. The simulation results show good agreement with experimental

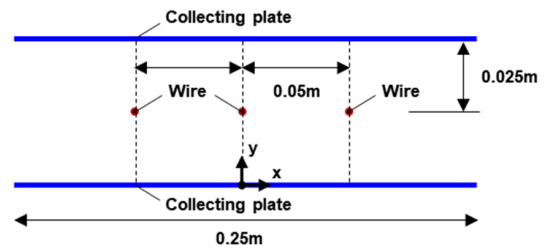
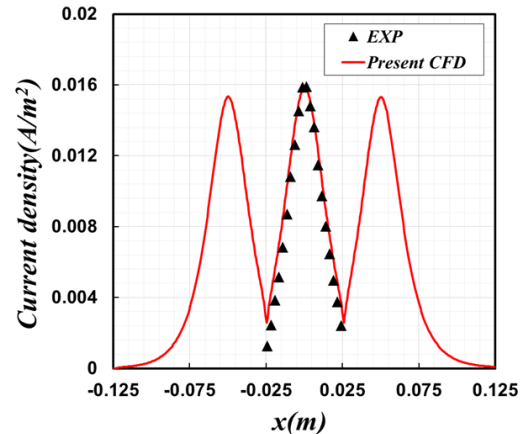
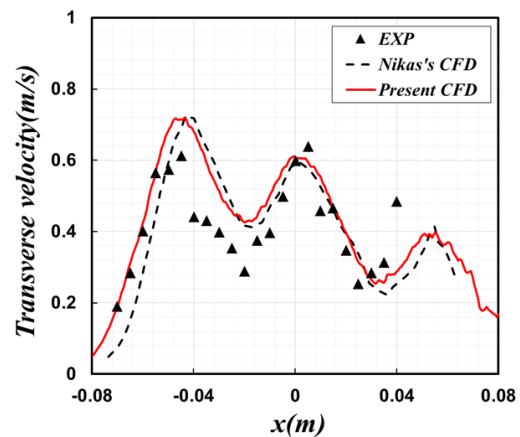


Fig. 5. Schematic of the electrostatic precipitator used by Parasram [15].



(a) Current density



(b) Transverse velocity of particles

Fig. 6. Comparison of (a) current density; (b) transverse particle velocity between present CFD and experimental data of Parasram [15].

data of Parasram as well as previous CFD results.

Finally, collection efficiency and corona current at wire according to applied voltage were compared with Kihm's [16] experimental data. Fig. 7 shows the schematic of the model of electrostatic precipitator used in Kihm's experiments. The electrostatic precipitator had eight wire electrode with diameter of 100 μm . Applied voltage on wire electrode is varied in the range of 6 to 13 kV. Inlet velocity of gas flow is 2 m/s. Fig. 8 shows the comparison of electric potential, ion current density, pressure, turbulent kinematic energy and particle trajectories between present CFD results and previous CFD results of Goo

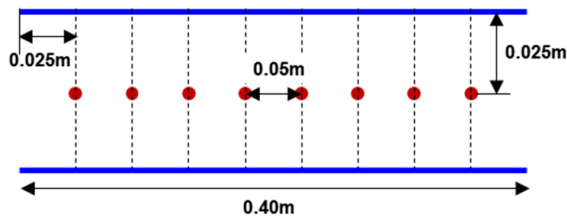


Fig. 7. Schematic of the electrostatic precipitator used by Kihm [16].

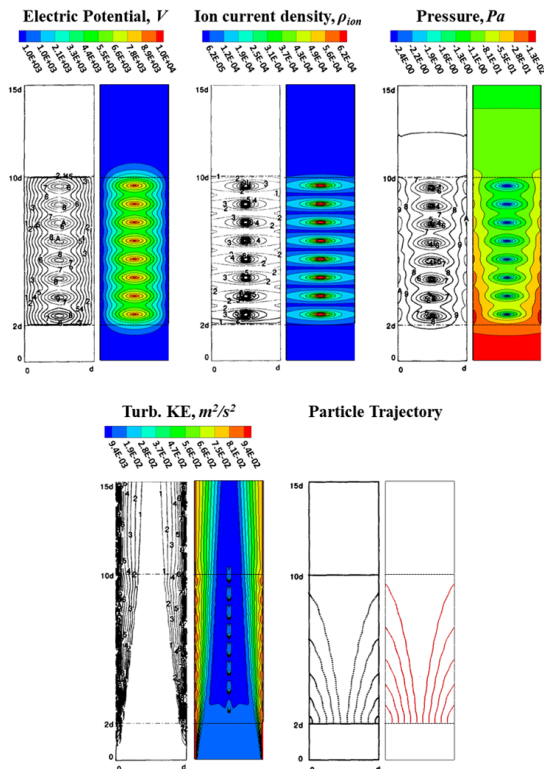
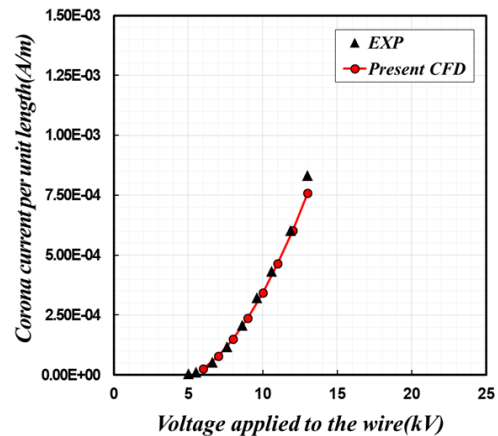


Fig. 8. Comparison of electric potential, ion current density, pressure, turbulent kinematic energy and particle trajectories between present CFD and previous CFD of Goo and Lee [8] for the applied voltage of 12.78 kV.

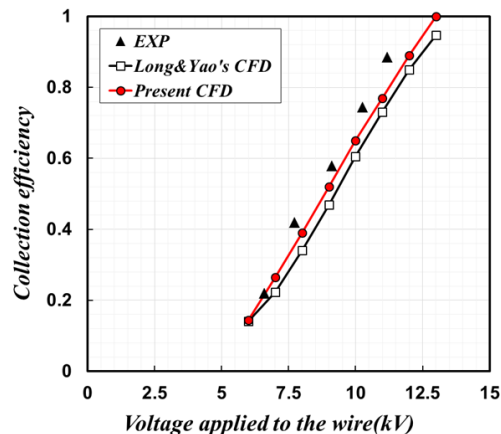
and Lee [8] on the applied voltage of 12.78 kV. The present CFD results of electrostatic precipitator, from electric fields to turbulent flow fields and particle trajectories, are very well matched with previous CFD results of Goo and Lee as shown in Fig. 8. Fig. 9 shows the comparison of corona current at wire and collection efficiency of electrostatic precipitator between present CFD and experimental data of Kihm. In Fig. 9(a), the increase in corona current per unit length with respect to change in applied voltage is very consistent with experimental data as well as CFD data of Long and Yao [13]. Also collection efficiency of electrostatic precipitator with respect to applied voltage is well predicted with experimental data of Kihm.

3.2 Effect of staggered arrangement of wire electrode

Based on electrostatic precipitator model used in Kihm's ex-



(a) Corona current per unit length of wire



(b) Collection efficiency

Fig. 9. Comparison of (a) corona current; (b) collection efficiency between present CFD and experimental data of Kihm [16].

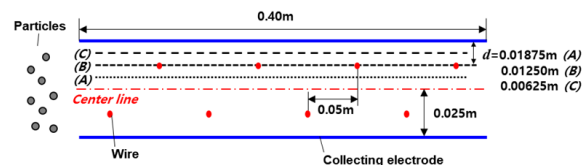
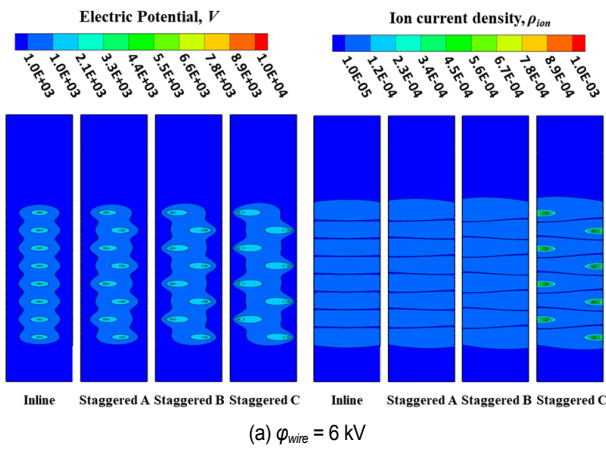


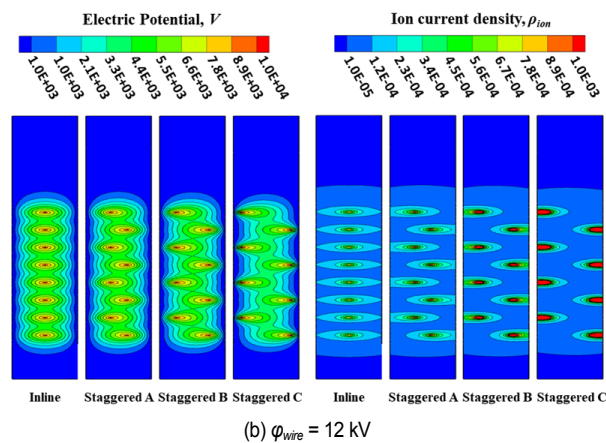
Fig. 10. Schematic of the electrostatic precipitator with staggered arrangements.

periment, the staggered arrangement of wire electrode was considered in Fig. 10. The design variable for the staggered arrangements of wire electrodes is the distance (d) between wire to collecting plate in y axis and its center is same as the center of electrostatic precipitator. d considered in staggered arrangement is 0.01875 m, 0.01250 m, and 0.00625 m, and is named as staggered A, B, and C, respectively.

Fig. 11 shows the comparison of contours of electric field in electrostatic precipitators for inline and staggered arrangements when applied voltage is (a) 6 kV and (b) 12 kV. As the applied voltage on wires increases, the gradient of electric potential around wires also increases. As d decreases, the



(a) $\phi_{wire} = 6 \text{ kV}$



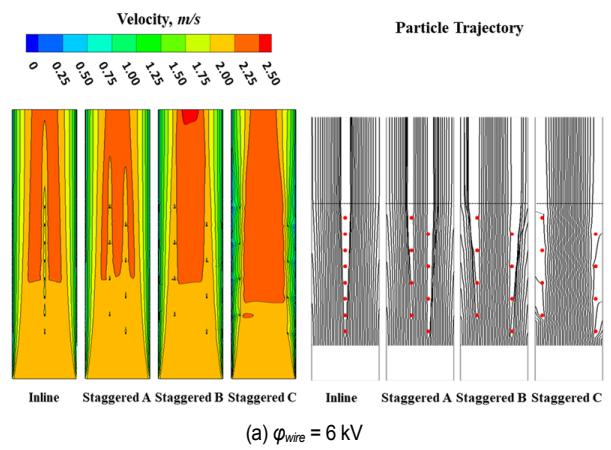
(b) $\phi_{wire} = 12 \text{ kV}$

Fig. 11. Contours of electric field in electrostatic precipitator with wire arrangements when applied voltage is (a) 6 kV; (b) 12 kV.

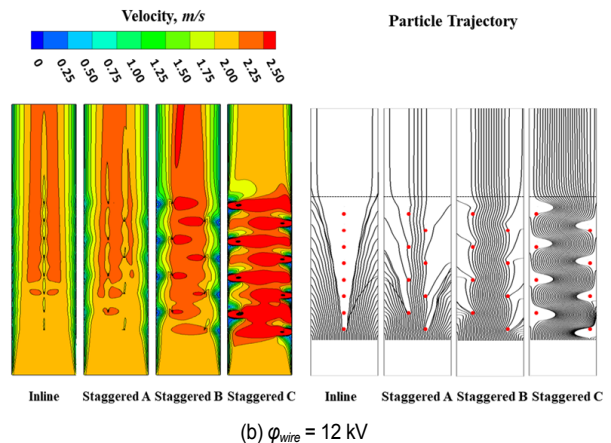
electric potential toward collecting plate is rapidly decreased. However the electric potential to the center line is slowly decreased. These results show that the strong electric strength is formed in electrostatic precipitator with increasing applied voltage on wires and decreasing d . The ion current density on wires is set to a value that satisfies the corona onset condition.

As the applied voltage increases, ion current density around wires also increases. As d decreases, the ion current density on wires also increases. These results show that the ion current density for corona onset increases due to increasing of electric strength on wires and decreasing d . The changes in the electric potential and ion current density affect the charging and coulomb force on the particles.

Fig. 12 shows the contours of velocity and trajectories of particles when applied voltage is (a) 6 kV and (b) 12 kV. Red color dots in the particle trajectory indicate wire electrodes. When the applied voltage is 6 kV, change of flow field by ionic wind is insignificant. Therefore transverse velocity forward to collecting plate is low in inline arrangement. However, as d decreases, the velocity gradient increases due to increasing ionic wind and turbulence effect. Secondary flow by ionic wind is observed in staggered C. And transverse velocity of particles becomes high with decreasing d . When the applied voltage is 12 kV, the sec-



(a) $\phi_{wire} = 6 \text{ kV}$



(b) $\phi_{wire} = 12 \text{ kV}$

Fig. 12. Contours of velocity and particle trajectory in electrostatic precipitator with wire arrangements when applied voltage is (a) 6 kV; (b) 12 kV.

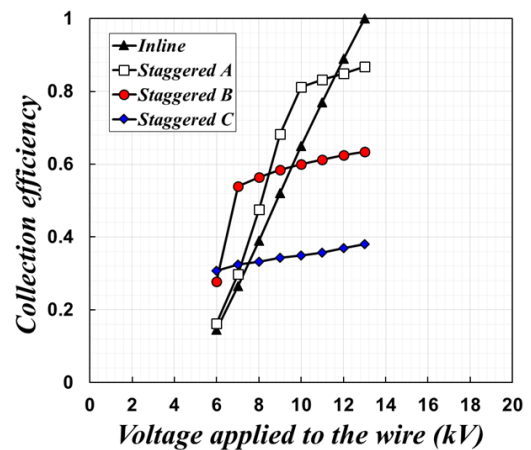


Fig. 13. Variation of collection efficiency with various applied voltage and wire arrangements.

ondary flow by ionic wind is observed in all arrangements due to the increasing electric force in electrostatic precipitator. Most of the particles passing between wire and plate were collected whereas particles passing between two vertical wire arrays penetrate the electrostatic precipitator. As d decreases, number of particles passing between two vertical wires arrays also

increases. These results affect the collection efficiency of electrostatic precipitator.

Fig. 13 shows the variation of collection efficiency with respect to applied voltage on wires and wire arrangements. Staggered A improves the collection efficiency when the applied voltage is less than 11 kV compared with the inline arrangement. If the applied voltage is higher than 11 kV, the increase of the collection efficiency is drastically reduced, and the collection efficiency is less than that of the inline arrangement. In case of staggered B, the collection efficiency at 6 kV is increased by more than twice, but the point which the increase of the collection efficiency is reduced occurs at the applied voltage lower than staggered A. In case of staggered C, collection efficiency at 6 kV has the highest value among all cases, but the increase of collection efficiency has the smallest value in all range of applied voltage. Staggered arrangements improve the collection efficiency in comparison to inline arrangement in low voltage conditions. However, the collection efficiency decreases in high voltage condition because the electric force applied on the particles passing between two vertical wire arrays is canceled out by both side wires.

4. Conclusions

In this simulation, the validity of numerical model was secured through comparison with previous experimental data. And the effects of wire arrangement in electrostatic precipitators are investigated in terms of electrohydrodynamic characteristics and particle motions. As d decreases, ion production increases and the effect of secondary flow is strongly affected. Number of particles passing between two vertical wires arrays increase. As applied voltage on wires increases, corona current increases by high electric strength and the effect of secondary flow to gas flow field is strongly affected. For low voltage condition, the staggered arrangement of wire electrodes caused the turbulent effect near the collection plate so that the collection efficiency increases more than that in case of inline arrangement. However, collection efficiency decreases in high voltage condition because of flow characteristics caused by arrangements and electric force applied in the space between two vertical wire arrays. If low voltage condition is to be used in electrostatic precipitators due to the limited conditions, the design of the arrangement of wire electrodes could contribute to improve the collection efficiency of electrostatic precipitators.

Acknowledgments

This work was supported by the National Research Foundation of Korea (NRF) grant, which is funded by the Korea government (MSIT) (No. NRF-2017R1A2B3004883 and No. 2019R1A5A808320111).

Nomenclature

ρ : Gas phase density (kg m^{-3})

u_k : Velocity component in x_k direction (m s^{-1})
 x_k : Coordinate in tensor notation (m)
 μ : Dynamic viscosity ($\text{kg m}^{-1}\text{s}^{-1}$)
 μ_t : Turbulent viscosity ($\text{kg m}^{-1}\text{s}^{-1}$)
 P : Pressure (Pa)
 F_e : Electric body force (N m^{-3})
 k : Turbulent kinetic energy ($\text{m}^2 \text{s}^{-2}$)
 ε : Turbulent dissipation rate ($\text{m}^2 \text{s}^{-3}$)
 C, C_1, C_2 : Constants of turbulent model
 $\sigma_k, \sigma_\varepsilon$: Constants of turbulent model
 φ : Electric potential (V)
 ρ_{ion} : Ion current density (C m^{-3})
 ε_0 : Air permittivity ($\text{C}^2 \text{N}^{-1} \text{m}^{-2}$)
 E_k : Electric strength (V m^{-1})
 K_{ion} : Ion mobility ($1.8 \times 10^{-4} \text{ m}^2 \text{V}^{-1} \text{s}^{-1}$)
 D_e : Ion diffusivity ($4.11 \times 10^{-6} \text{ m}^2 \text{s}^{-1}$)
 δ : Relative density of air
 r : Radius of wire electrode (m)
 E_s : Electric strength at wire (V m^{-1})
 u_p : Particle velocity (m s^{-1})
 C_D : Drag force coefficient
 ρ_p : Particle density (kg m^{-3})
 q_p : Particle charge (C)
 m_p : Particle mass (kg)
 d_p : Particle diameter (m)
 e : Charge on an electron ($1.6 \times 10^{-19} \text{ C}$)
 k_b : Boltzmann's constant (J K^{-1})
 K_p : Particle dielectric constant
 d : Distance between wire to collecting plate (m)

References

- [1] W. C. Hinds, *Aerosol Technology: Properties, Behavior, and Measurement of Airborne Particles*, John Wiley & Sons (2012).
- [2] P. Cooperman, A new theory of precipitator efficiency, *Atmospheric Environment*, 5 (1971) 541-551.
- [3] G. Leonard, M. Mitchner and S. A. Self, Particle transport in electrostatic precipitators, *Atmospheric Environment*, 14 (1980) 1289-1299.
- [4] J. R. McDonald, W. B. Smith, H. W. Spencer III and L. E. Sparks, A mathematical model for calculating electrical conditions in wire-duct electrostatic precipitation devices, *J. Appl. Phys.*, 48 (1977) 2231-2243.
- [5] S. H. Kim, H. S. Park and K. W. Lee, Theoretical model of electrostatic precipitator performance for collecting polydisperse particles, *J. Electrostat.*, 50 (2001) 177-190.
- [6] K. S. P. Nikas, A. A. Varonos and G. C. Bergeles, Numerical simulation of the flow and the collection mechanisms inside a laboratory scale electrostatic precipitator, *J. Electrostat.*, 63 (2005) 423-443.
- [7] J. H. Goo and J. W. Lee, Stochastic simulation of particle charging and collection characteristics for a wire-plate electrostatic precipitator of short length, *J. Aerosol Sci.*, 28 (1997) 875-893.

- [8] W. B. Smith and J. R. McDonald, Development of a theory for the charging of particles by unipolar ions, *J. Aerosol Sci.*, 7 (1976) 151-166.
- [9] H. J. White, Particle charging in electrostatic precipitation, *Trans. AIEE.*, 70 (1951) 1186-1191.
- [10] K. Adamiak and P. Atten, Numerical simulation of the 2-D gas flow modified by the action of charged fine particles in a single-wire ESP, *IEEE Trans. Dielectr. Electr. Insul.*, 16 (2009) 608-614.
- [11] K. Adamiak, Numerical models in simulating wire-plate electrostatic precipitators: A review, *J. Electrostat.*, 71 (2012) 673-680.
- [12] P. A. Lawless, Particle charging bounds, symmetry relations and analytic charging rate model for the continuum regime, *J. Aerosol Sci.*, 27 (1996) 191-215.
- [13] G. W. Penney and R. E. Matick, Potentials in D-C corona fields, *Trans. Am. Inst. Elect. Eng.*, 79 (1960) 91-99.
- [14] N. Parasram, Particle motion in electric precipitators, *Ph.D. Thesis*, Imperial College of Science, Technology and Medicine (2001).
- [15] K. D. Kihm, Effects of nonuniformities on particle transport in electrostatic precipitators, *Ph.D. Dissertation*, Stanford University, Stanford, CA (1987).
- [16] K. Luo, Y. Li, C. Zheng, X. Gao and J. Fan, Numerical simulation of temperature effect on particles behavior via electrostatic precipitators, *Applied Thermal Engineering*, 88 (2015) 127-139.
- [17] Q. Lu, Z. Yang, C. Zheng, X. Li, C. Zhao, X. Xu, X. Gao, Z. Luo, M. Ni and K. Cen, Numerical simulation on the fine particle charging and transport behaviors in a wire-plate electrostatic precipitator, *Advanced Power Technology*, 27 (2016) 1905-1911.
- [18] Z. Long and Q. Yao, Evaluation of various particle charging models for simulating particle dynamics in electrostatic precipitators, *Journal of Aerosol Science*, 41 (2010) 702-718.



Ho Yeon Choi received his B.S. degree from Dong-A University, Korea, in 2014, and his M.S. degree from Pusan National University, Korea, in 2016. He started attending Pusan National University for the Ph.D. program under the supervision of Professor Man Yeong Ha. His research interests are focused on numerical simulation on electro-hydrodynamics in electrostatic precipitator.



Yong Gap Park received his B.S. degree from Pusan National University, Korea, in 2008, his Ph.D. degree from Pusan National University, Korea, in 2014. Dr. Park is currently a Professor at the School of Mechanical Engineering, Changwon National University in Changwon. His research interests are focused on natural convection, heat exchanger and computational fluid dynamics.



Man Yeong Ha received his B.S degree from Pusan National University, Korea, in 1981, his M.S. degree from Korea Advanced Institute of Science and Technology, Korea, in 1983, and his Ph.D. degree from Pennsylvania State University, USA in 1990. Dr. Ha is currently a Professor at the School of Mechanical Engineering at Pusan National University in Busan, Korea. He served as Editor of the Journal of Mechanical Science and Technology. He is a member of Honorary Editorial Advisory Board of the International Journal of Heat and Mass Transfer. His research interests are focused on thermal management, computational fluid dynamics, and finite volume method using hybrid scheme.